An Analysis of Charge Transfer Efficiency Noise on Proton-Damaged CCDs for the Hubble Space Telescope Wide Field Camera 3

Scott D. Johnson[a] and Augustyn Waczynski[a] and Elizabeth Polidan[a] and Paul Marshall[b] and Robert Reed[c]

[a]Global Science & Technology, NASA/Goddard Space Flight Center, Greenbelt,MD 20771 USA
[b]NASA/Goddard Space Flight Center, Brookneal,VA 24528 USA
[c]NASA/Goddard Space Flight Center, Greenbelt, MD 20771 USA

ABSTRACT

Proton induced charge transfer efficiency (CTE) degradation has been studied in the large format charge-coupled device (CCD) flight-like candidates for Wide Field Camera 3 for the Hubble Space Telescope. These detectors were irradiated with different proton fluences. This paper focuses on the statistical nature of CTE degradation due to damage on one of the irradiated devices with exceptional initial CTE characteristics. In radiation damaged CCDs, CTE noise can be the dominant noise component. In contrast to other noise sources, CTE noise has a component of fixed pattern noise that can be removed by the appropriate calibration technique. A large set of data was acquired and analysis of it confirms the expectation that CTE damage is a local phenomenon and it varies widely across the CCD surface. Possible mitigation solutions and their practicality are discussed in some detail.

Keywords: CCD, Proton damaged CCD, CTE, CTE noise, scientific CCD, WFC3, HST

1. INTRODUCTION

The Detector Characterization Laboratory and the Radiation Effects and Analysis Group at NASA Goddard Space Flight Center have measured the radiation characteristics of the Hubble Space Telescope (HST) Wide Field Camera 3 (WFC3) CCD detectors. Marconi Applied Technologies Ltd. (Marconi) CCD43 flight-like detectors were irradiated at the U.C. Davis Crocker Nuclear Laboratory with different proton fluences ranging from 1×10^9 protons/cm^2 to 5×10^9 protons/cm^2 at a single energy of 63.3 MeV which represent an equivalent dosage of 1 to 5 years in an HST environment, respectively.[1] The dosimetry error was less than 10%.

The CCD used for this paper is a Marconi CCD43 flight-like device, irradiated to an equivalent 2.5 years HST environment dose. Further discussion of the irradiation of the WFC3 devices can be found in Waczynski[1] where Marconi CCD44s were exposed to radiation in a similar manner to the CCD43s.

It has been shown in the experience of other missions (eg. the Space Telescope Imaging Spectrograph (STIS) and the Wide Field Planetary Camera 2 (WFPC2)) and in our own radiation testing that, for WFC3 like conditions, serial CTE is an order of magnitude better than parallel charge transfer efficiency (CTE). For that reason, the focus of this paper is almost entirely on parallel CTE and this is the CTE discussed herein.

It is well established that CTE degradation results in reduced photometric capability. Less studied is the effect of CTE noise. CTE noise on a proton damaged device can be, in certain instances, a dominant noise component.[1] Therefore a thorough understanding of CTE noise is important.

The CTE noise considered here has two components. One is the noise generated when the charge interacts with bulk traps. This is a random noise that is small compared to the average shot noise (in all but the most

Further author information: (Send correspondence to S.D.J.)
S.D.J.: E-mail: johnson@cte.gsfc.nasa.gov, Telephone: 1 301 286 3673

severely damaged devices). The other source of CTE noise, and the primary focus of this paper, is a fixed pattern CTE noise that is correctable in principle. As a charge packet travels across the CCD, the amount of loss depends on the particular path. Therefore originally equal packets are measured at the CCD output as having different sizes and thus we have CTE noise. Three different methods were used in the attempt to mitigate the CTE: optical flat bias, charge injection, and a local CTE algorithm. The first two methods are discussed briefly here along with a more in depth discussion of the third method and its resulting effects on CTE noise.

2. BACKGROUND

Radiation damage of a CCD in the WFC3 environment consists of damage to the oxide and damage to the bulk layer.[2] Damage to the oxide effects the surface dark current which can be alleviated using MPP mode if available. Energetic particle collisions with a bulk silicon device such as a CCD dislodge silicon atoms which lead to defects in the lattice structure. The defects act as carrier generation and trapping centers in the CCDs. The dominant trap type is the phosphorus vacancy complex (E-center) though other trap types may also be present.[2] These trapping centers are responsible for CTE degradation and are distributed throughout the device.

Distribution of these traps across the CCD array is random; however, significant non-uniformity may exist between different areas of the device and even between different sections of the same column. As a charge packet travels along the column, it may be losing charge in a highly non-uniform fashion. The same packet may lose different amounts of charge depending if it is located before or after a major trapping area. It is typical to assume the same CTE for a whole device. As long as the CTE is good (e.g. an undamaged CCD) this is a reasonable approximation. However, for a radiation damaged device it is believed that better results could be obtained by calibrating the local CTE for each column, group of pixels, or each pixel. Evidence of non-uniform CTE can be easily spotted by looking at the stacking plots for ^{55}Fe tested radiation damaged CCDs (see figure 1). As one moves farther from the serial register readout, the single event line not only shows that signal magnitude is lower (slope in the line) but also that the amount of lost charge is different from event to event (broadening of the line). Closer to the serial register the spread in the line is close to that predicted by fano noise while at the end it widely exceeds any expectation for CTE related random noise. The increased uncertainty, beyond that of fano noise, read noise and CTE random noise must be due to another reason. It is assumed that excessive noise observed in the data is due to a non-uniform distribution of the trapping centers, further referred to as a 'fixed pattern CTE noise'.

Waczynski[1] has previously confirmed a fixed pattern to CTE noise using the first pixel response (FPR) method on devices (CCD44) similar to the flight devices to be used for WFC3.[1] It was shown that a good correlation existed for several FPR images where CTE noise was dominant. This led to the conclusion that there was a fixed pattern to the CTE noise.

A noise relationship for CCDs that have been exposed to ^{55}Fe can be expressed as

$$\sigma_{CCD}^2 = \sigma_{readnoise}^2 + \sigma_{fanonoise}^2 + \sigma_{CTEFP}^2 + \sigma_{CTE}^2 \,, \tag{1}$$

where σ_{CTEFP} is the fixed pattern CTE noise and σ_{CTE} is a random CTE noise factor. Both of these CTE noise factors depend on the position in the CCD and therefore the above noise relationship will also be position dependent. For the WFC3 detectors with flight-like operation conditions,[1] $\sigma_{readnoise}$ is very small at approximately $2.0e^-$. Fano noise[3] is $\sqrt{(0.11 \times signal)} = 13.3e^-$. To estimate the random CTE noise component, the following equation[3] is used.

$$\sigma_{CTE} = \sqrt{2 \times CTI \times N_p \times signal} \tag{2}$$

The CTE noise for this device (2.5 years damage with a CTE of 0.99996 which is a function of the density used for this experiment) is from slightly greater than $0e^-$ at the readout to approximately $16e^-$ at the position furthest from the readout on our devices. N_p is the number of pixel transfers.

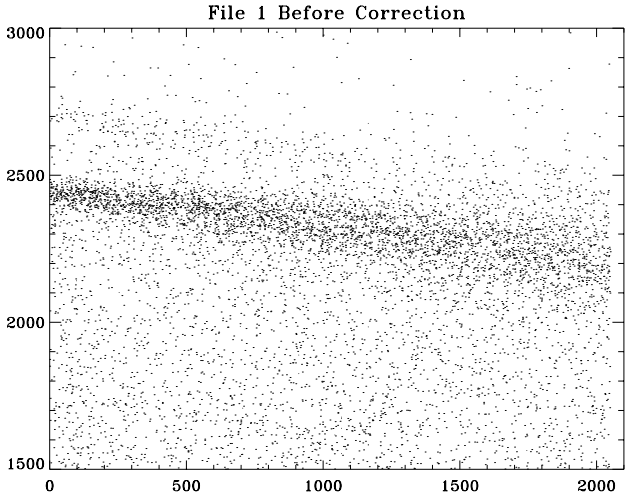

Figure 1. This is a stacking plot before any CTE correction. Note that near the serial readout the fano noise dominates, but beyond that CTE noise starts to dominate.

Fixed pattern CTE noise is by far the dominant noise in radiation damaged CCDs. Previous experimental data shows that it follows the relationship[1]

$$\sigma(CTI) \simeq k \times CTI \times N_p \times mean(signal)\,, \tag{3}$$

where N_p is the number of parallel transfers.

Typical traps caused by space radiation may have re-emission time constants significantly longer than CCD line readout when the CCD operates at low temperatures.[2] Once a trap is filled with charge, it becomes "invisible" to other charge packets until it is emptied by re-emission. For this reason CTE noise may vary depending on the type of image. For very dense, high intensity images it may be negligible; but it may be severe for sparse, low signal, low background astronomical fields.

3. DEVICES

The detector used for this experiment is a Marconi CCD43 front-side illuminated flight-like detector (the flight devices are back-side illuminated). It has a 2051x4096 image size with a $15\mu m$ x $15\mu m$ pixel size. This device also has a mini-channel and can run in multiphase pinned (MPP) mode. This detector does not have frame transfer capability therefore no First Pixel Response (FPR) test could be performed. It has a single parallel register and single, split serial register terminated by amplifier on each side. That allows the reading of the device simultaneously by both outputs or by a single one. The single image register complicates the application of the FPR method for parallel CTE determination, therefore EPER and ^{55}Fe have been used instead. Most of the results presented here were obtained with ^{55}Fe method.

In order for the results to be meaningful and comparable to work by others it is necessary to specify all measuring conditions that are relevant to CCD operations.[1] In this case, measurements were run at a temperature of $-83°C$ with a readout speed of 100 kHz, simultaneously by both amplifiers. That resulted in a residency time of 20 ms under image phase 2 and a $40\mu s$ residency time for phases 1 and 3. All data are acquired with a device in full inversion (MPP mode). The average density of single events per column (2051 pixels) was approximately 10 for this experiment.

4. EXPERIMENTAL AND ANALYTICAL PROCESS

In order to mitigate fixed pattern CTE noise, two experimental methods were employed. The first method was an optical bias. The detector was exposed to a flat field of low intensity (approximately $35e^-$ to approximately $1000e^-$) and then CTE measurements (in this case using ^{55}Fe) were performed on the device. The second method was to use an injected line of charge at different line distances apart (25 lines to 500 lines). In this method the lines were injected onto a CCD and then the device was exposed to ^{55}Fe. The lines were injected at approximately the same speed as the readout. These two methods are discussed only briefly, and with preliminary results.

For the analytic approach the goal was to use a map of CTE values covering local regions instead of just one CTE value. It was hoped that a calibration using a map of CTE values would reduce the CTE noise. Two slightly different approaches were used to correct for the effects of local CTE. After correcting for local CTE, the noise of the resulting images was compared to the noise of an image corrected using one global CTE value. A single CTE number is the typical way astronomical images are corrected for the effects of CTE degradation.

A large number (300) of ^{55}Fe images with approximately 10 single event per column was acquired to build a data set with a sufficient number of hits per column to produce a local CTE map using either of the two methods. The columns were combined from each of the 300 files to produce one column with a reasonable number of hits. In other words, 300 of column 1 were combined, 300 of column 2 were combined, etc. For this investigation 500 columns of one side of the device were used for both the local CTE map and the test files.

Once the data set was created the first of the two methods, wherein a different CTE value is used for each column (the column CTE method) was applied to a test data set. A stacking plot was created for each column, a best fit to the single event line produced the CTE for each column. The row by row charge loss was determined to produce a correction array for each column. The arrays were assembled to construct a map of correction values for the damaged image. Each of 10 test images was multiplied by the correction map. The 10 test images were combined to get a sufficient statistical sample of the noise.

To further refine the process the second method calculates a local CTE at different points along each column, creating a map of CTE values. The correction is applied to the test image, and the respective CTE noises are compared. The goal is to show that the degree of noise improvement depends on the accuracy of the CTE characterization. Ideally, CTE should be measured for each pixel at different intensities. Using the present technique of ^{55}Fe with a low number of events per column, the CTE was determined for a group of 25 pixels. Further refinement requires an impractical number of exposures. To estimate the CTE for a given pixel it would be necessary to collect a large enough set of data which, when combined, would ensure a high probability of each pixel receiving at least 30 single events. At the same time, to avoid interaction between single events, the number of hits per column should be very low because at $-83°C$ the trap re-emmision time constant can be in the range of seconds.[1] The above requirements combined together lead to the need to acquire an impractical number of files to evaluate CTE per single pixel. For that reason the experiment was limited to groups of 25 pixels, just to demonstrate that fixed pattern CTE noise is correctable.

To create the local CTE map, each column is processed separately. Along the column, the mean of each bin of 25 pixels is determined (see example for one column in figure 2). A linear fit produces an extrapolation of the signal level at the readout amplifier. All other values along the column are normalized to this signal level. These normalized values are assembled into a map of the array to use for correction. Each of 10 test images was multiplied by the correction map. The 10 test images were combined to get a sufficient statistical sample of the noise.

5. RESULTS

A number of different CTE mitigation schemes was tried including the use of a optical bias, charge injection, and the correction scheme described above. To mitigate CTE an optical bias was applied and the ^{55}Fe method was used for the CTE measurement. For small flat field biases, noise near the serial readout is dominated by fano noise as is in a raw image. Near the furthest position from the readout the CTE noise is dominant. For larger flat field biases the shot noise dominates near the readout and at the furthest position from the readout.

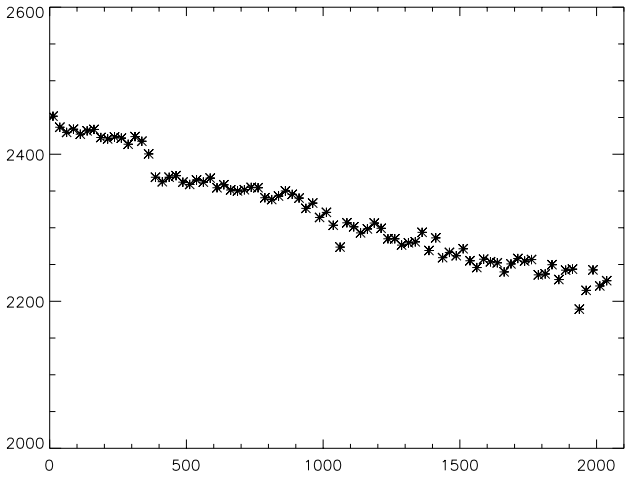

Figure 2. This sample single event line from one column binned in groups of 25 rows illustrates the charge loss along this column. Note the areas were the CTE is the same for some number of rows. Also notice drops near various trapping centers. It can be seen clearly that this data captures the local behavior along this column of the traps.

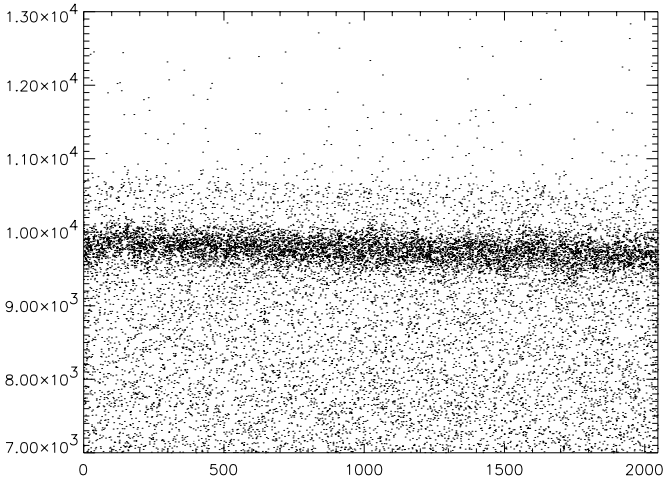

Figure 3. This is a stacking plot after an optical bias. Note that the gain in this particular plot is different from that of all other plots herein.

For the device used in this experiment a flat field bias of $700e^-$ is sufficient to give a CTE close to pre-radiation status. At this flat field level the shot noise of $26e^-$ is less than the observed CTE noise on an uncorrected device. Since this noise is practically the same from the readout to the furthest position from the readout (see figure 3) it can be concluded that CTE noise is mitigated to at least below the shot noise level. The penalty for this mitigation is higher noise near the readout.

Preliminary investigation of CTE mitigation using lines of injected charge shows good improvement of CTE noise close to the injected line (see figure 4). Charge injection offers considerable benefit over optical biases because of its lower noise characteristics.

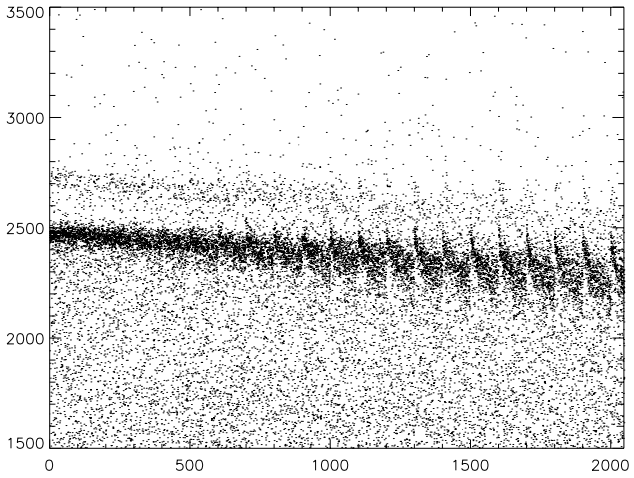

Figure 4. This shows a stacking plot with a $20ke^-$ charge injected line every 100 rows. Note that the noise close to the injected line is small (a little greater than fano noise) but farther from the injected line the CTE noise has increased. The 100 line injection is used here to illustrate this increase in CTE noise away from the injected line because this is not easy to observe with more closely spaced lines. Note the very short re-emission time here.

Lastly the correction algorithms were used to mitigate CTE and CTE noise. In all cases, the single event line is restored to the original signal level, as can be seen by comparing the stacking plots with that of the uncorrected image (see figure 1). The stacking plot of the image before correction is seen in figure 1. Figure 5 shows the corrected image's stacking plot after using a correction based on one global CTE number. In figure 6 it is seen that using a CTE value for each column in the correction reduces the CTE noise. A further reduction in noise is observed in figure 7 where a local CTE correction has been applied to the image. Note that in these cases near the readout the dominant noise is fano noise which is significantly less than the shot noise at the readout if the optical bias was used to mitigate CTE noise.

CTE noise for the different correction schemes is compared in figure 8. Correcting for CTE with one global number produces a signal to noise ratio at the position furthest from the readout of approximately 30. The signal to noise ratio increases to 35 if CTE is corrected column by column. Correcting for local CTE gives a modest increase in signal to noise of 37. While not a substantial improvement, it does verify that this CTE fixed pattern noise is correctable. Below is a discussion of some limiting factors to these algorithms.

6. DISCUSSION

Radiation caused CTE degradation results in signal reduction and in increased inaccuracy. Inaccuracy can be easily observed in ^{55}Fe stacking plots, however it is not reflected in the baseline. In this paper it is called fixed pattern CTE noise since, like an ordinary noise, it reduces effective signal to noise ratio. As has been shown experimentally, CTE noise can be significantly reduced by estimating local CTE for a given column, group of pixels or pixel. The relatively modest improvement observed could be due to the fact that an ultimate resolution of the CTE mapping was not achieved. However, it is also possible that other limiting factors were involved.

It should be noted that the experiment described here maps CTE for a specific application and for a specific type of image. As soon as the image changes the CTE map may change and the calibration would need to be repeated. Also, in a space environment, radiation damage is not static and the calibration map would need to be periodically updated. Considering the effort it takes to produce a single calibration map, this whole approach can be treated only as a proof of concept. It is quite possible that a better approach to CTE calibration can be found. A possible candidate would be to map traps by a charge or pocket pumping method[4] and deriving CTE

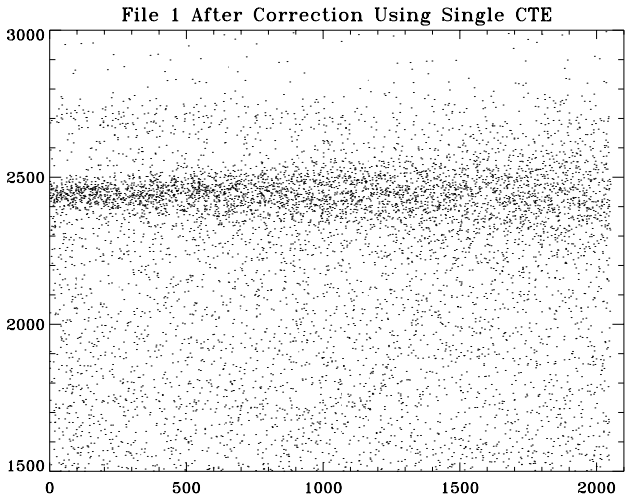

Figure 5. This is a stacking plot after standard CTE correction using one global CTE number.

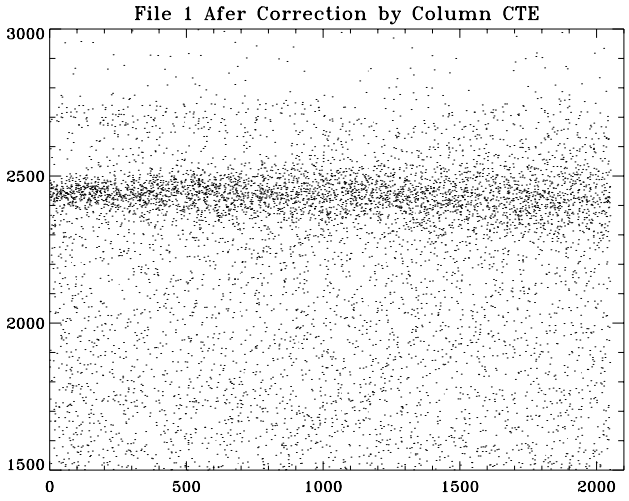

Figure 6. This is a stacking plot after column by column CTE correction. Note the noise near the serial readout is still dominated by fano noise, yet the point furthest from the readout has less noise than if the image is corrected using one global CTE number.

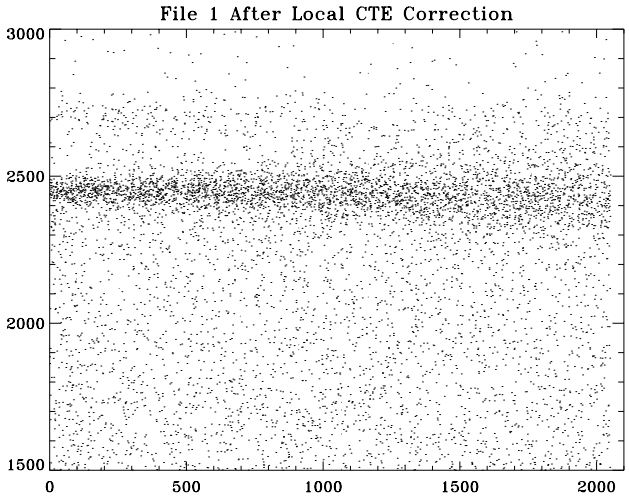

Figure 7. This is a stacking plot after local CTE correction. Note the noise band is slightly tighter than if the column by column method is applied to this test image. For the final statistical results ten corrected files were combined, this is an example of only one of those files.

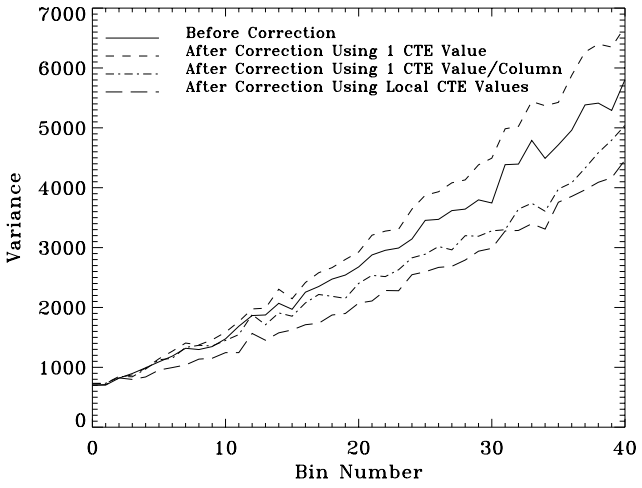

Figure 8. This is a comparison of noise (variance in ADU) from CTE (includes all noise components) before any correction is applied, after correcting for CTE with one number, after correcting using different CTEs per column, and after correcting with local CTE.

properties by modeling. The scope of this work did not allow for full comparison of CTE correction methods with CTE mitigation techniques like fat bias and injection of a sacrificial line of charge. Initial results indicate that CTE correction could be used to supplement other mitigation techniques.

7. CONCLUSION

It has been observed that noise in data collected on radiation damaged devices is significantly higher than expected from standard assumptions. It is assumed that this increased noise is caused by non-uniformity in the damage due to radiation. This results in a fixed pattern CTE noise. This pattern can be calibrated and corrected for. An approach to estimate local CTE has been shown as well as the resulting reduction in CTE noise. The relatively modest reduction in noise arises from the experiment's limitations. Other approaches for CTE mitigation have been briefly considered, including optical flat bias (fat zero) and electrical charge injection. As the level of the optical bias increases so does the CTE, since charge traps are filled. However, noise dependency is more complicated. Initially, CTE noise gets reduced as CTE improves, it reaches a minimum and increases again due to shot noise of the bias and its spatial non-uniformity. More promising is the mitigation technique where a single line (row) of charge is shifted in front of the signal packets to temporarily fill charge traps. Significant reduction in CTI has been observed for events immediately following the line of charge, however, charge re-emitted from the traps increases baseline noise. These effects have not been quantified with sufficient accuracy and further work in this area is needed.

It is important to note that the proposed CTE correction approach may improve photometric accuracy but it has no impact on floor noise, since the image is not reconstructed but only corrected. This, in itself, may be a significant limitation and other approaches and techniques may need to be explored to overcome it. Clearly, further work is needed in this area.

REFERENCES

1. A. Waczynski, E. J. Polidan, P. W. Marshall, R. A. Reed, S. D. Johnson, R. J. Hill, G. S. Delo, E. J. Wassell, and E. S. Cheng, "A comparison of charge transfer efficiency measurement techniques on proton damaged n-channel ccds for the hubble space telescope wide-field camera 3," *IEEE Transactions on Nuclear Science* **48**, pp. 1807–1814, 2001.
2. T. Hardy, R. Murowinski, and M. Deen, "Charge transfer efficiency in proton damaged ccd's," *IEEE Transactions on Nuclear Science* **45**, pp. 154–163, 1998.
3. A. Owens, K. J. McCarthy, A. Wells, W. Hajdas, F. Mattenberger, A. Zehnder, and O. Terekhov, "Measured radiation damage in charge coupled devices exposed to simulated deep orbit proton fluxes," *Nuclear Instruments & Methods in Physical Research Section A* **361**, pp. 602–610, 1995.
4. J. Janesick, *Scientific Charge Coupled Devices*, SPIE, Bellingham, WA, 2001.